Reverse Conduction of a 100 A SiC DMOSFET Module in High-Power Applications

R. A. Wood
U. S. Army Research Lab
2800 Powder Mill Road
Adelphi, MD, USA

D. P. Urciuoli
U. S. Army Research Lab
2800 Powder Mill Road
Adelphi, MD, USA

T. E. Salem
U. S. Naval Academy
105 Maryland Ave
Annapolis, MD 21402 USA

R. Green
U. S. Army Research Lab
2800 Powder Mill Road
Adelphi, MD, USA

***Abstract* - Numerous research efforts over the past few years have documented the enhanced capabilities that Silicon Carbide (SiC) offers over Silicon based power electronic devices. Additional research work has led to vast improvements in the manufacturing of SiC based components. As a result, SiC power electronic components, primarily diodes, are now readily available and this technology promises to have widespread market impact as more complex device structures are commercially realized. Recently, the development of a 1200 V 50 A SiC DMOSFET device and its use in a 100 A power module has been documented [1]. This paper extends that research work to report on the reverse conduction characteristics of the SiC DMOSFET and the system-level benefits for high-power applications that can be achieved by operating these devices in this manner. Experimental data is presented on the 100 A module consisting of two, 50 A SiC DMOSFETs and two, 50 A SiC JBS anti-parallel free-wheeling diodes used in a high-power bi-directional DC-DC converter during buck mode operation.**

I. INTRODUCTION

The design and development of electric and hybrid electric vehicles has been widely researched and documented, for example [2-4]. These vehicles afford unique challenges for power electronic systems such as reliable operation in a high-temperature environment while minimizing mass and volume [3]. In these vehicles, power electronics are used in inverter applications to directly drive the traction machines, and in DC-DC converters to efficiently manage power transfers between the energy storage system and the electric loads. This latter function of managing power transfer is typically realized using a bi-directional DC-DC converter [5-7]. Due to the power electronic devices used, most bi-directional converter topologies do not use a complementary switching scheme, which is a system-level inefficiency. A thorough overview on the specific challenges for bi-directional converters has recently been presented in which the need for suitable switching devices was highlighted [8-9]. To address these issues, a 50 A SiC DMOSFET has been developed and its use in a 400 A all SiC phase leg module has been proposed [10]. This work reports on the system-level efficiency improvements achieved by using the reverse conduction capabilities of the SiC DMOSFET. Both experimental and simulation data is presented for a 100 A module consisting of two, 50 A SiC DMOSFETs and two, 50 A SiC JBS anti-parallel free-wheeling diodes used in a high-power bi-directional DC-DC converter.

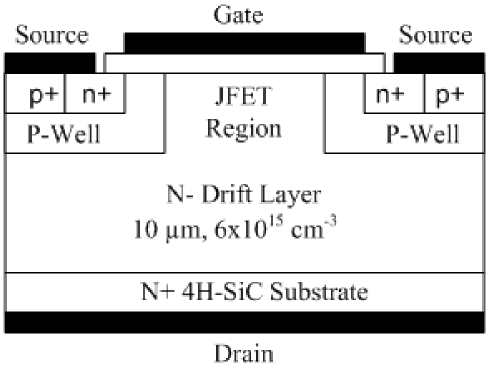

Figure 1: Simplified 1200 V SiC DMOSFET.

II. SIC DMOSFET MODULE

The SiC DMOSFET, shown in Fig. 1, is a vertically structured device that can conduct very large currents and block very high voltages during high-temperature operation. During forward operation, electrons flow laterally from the source through the inverted p-well and into the JFET region and then vertically into the drift layer and out through the drain contact. When the drain voltage polarity is negative, an intrinsic parasitic body diode formed by the p-n junction of the p-well and the n^- drift layer is forward-biased and conducts current. Reverse current conduction through the SiC DMOSFET is possible when the gate of the SiC DMOSFET is turned-on while the drain voltage polarity is negative. During reverse conduction, electron flow is from drain-to-source via the same path as described for forward

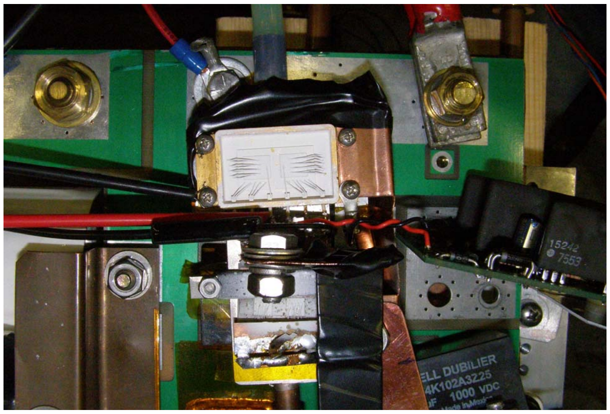

Figure 2: Picture of the 100 A SiC Module in the Bi-Directional Converter.

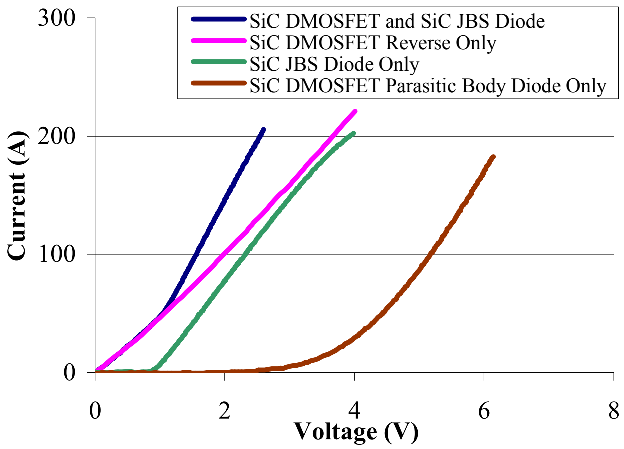

Figure 3: I-V Characteristics for the 100 A SiC Power Module at 25 °C.

conduction. Operating a MOSFET in reverse conduction while in a circuit is referred to as synchronous rectification and has been recently documented for a low-power SiC transistor [11-12].

The previously described 100 A SiC module shown in Fig. 2 had its current-voltage (I-V) characteristic curves measured by a Tektronix 371B high-power curve tracer. Fig. 3 shows the conduction characteristics of the SiC DMOSFET body diodes with a gate voltage of –10 V (DMOSFET turned off), the SiC JBS diodes only, and both the SiC JBS diodes and the SiC DMOSFETs turned on with a gate voltage of 15 V operating in reverse conduction. The gradual turn-on characteristic of the SiC DMOSFET body diode in comparison to the SiC JBS diode indicates that most of the current will flow through the SiC JBS diode path when the SiC DMOSFET is turned off. However, with the SiC DMOSFET turned on, the I-V characteristic indicates that at lower currents the SiC DMOSFET will have all of the flow until the SiC JBS diodes conduct at a reverse voltage of approximately 1.0 V. At each operating condition shown in Fig. 3, the product of voltage and current results in power loss in the device, and it is apparent that the minimum power loss always occurs when both the SiC MOSFET and the SiC JBS diode are available to conduct.

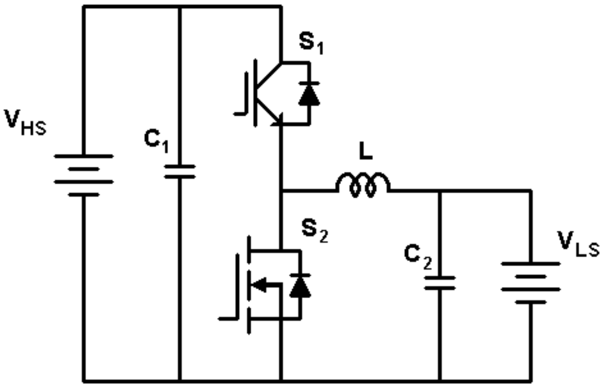

Figure 4: Bi-Directional Converter Circuit Used for Reverse Conduction of SiC DMOSFET.

III. TEST PROCEDURE

Fig. 4 shows a circuit for a bi-directional converter that can operate either in boost or buck mode. Both modes produce similar waveforms and losses on the switching devices. This circuit was operated in buck mode with a commercial IGBT as switch S_1 and the 100 A SiC DMOSFET module as switch S_2. To demonstrate efficiency gains possible through synchronous rectification, S_2 was operated in two different switching schemes. First, S_2 was turned off and the SiC JBS diode conducted all of the S_2 current. Then a complimentary switching scheme was utilized which allowed reverse conduction in the SiC DMOSFET while the SiC JBS Diode was also conducting. In this second scheme, a dead time of 4.8 µs between the gating of S_1 and S_2 prevented shoot-through of the high side power supply (V_{HS}).

The experimental bi-directional circuit was operated at a switching frequency of 10 kHz and pulse widths for S_1 and S_2 were 45.2 µs. Gate signals for both switches were 14.7 V and –7.6 V for turn on and turn off, respectively. The magnitude of V_{HS} was varied to adjust the amount of current and power that flowed through the circuit. The SiC DMOSFET module (S_2) was mounted on a liquid-cooled heat exchanger and was cooled by propylene glycol and water.

As shown in Fig. 5, thermal images of the SiC DMOSFETs and the SiC JBS diodes under test were taken to determine the amount of power loss for each device. This was accomplished by first characterizing the temperature rise of the module components during DC operation for which voltage drop and current directly result in thermal power. Then, during operation of the module in the bi-directional converter, temperature rise measured by the infrared camera was correlated to the DC data to obtain the thermal power loss in each device.

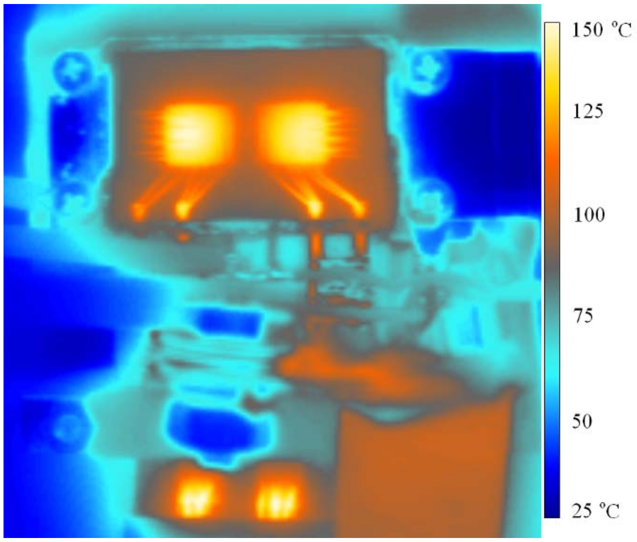

Figure 5: Thermal Image of Module at 23 kW Operation and 80 °C Coolant MOSFETs on Top, Diodes on Bottom

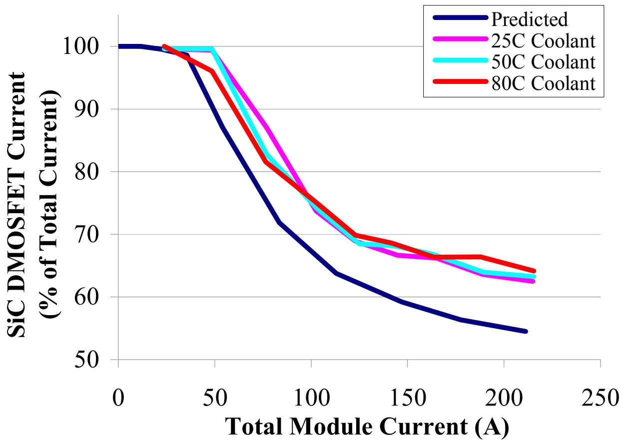

Figure 6: Current Sharing Between Devices During Reverse Conduction.

IV. SIMULATION RESULTS

To predict module performance during operation, current sharing among the devices needs to be known. Utilizing the I-V characteristics of the devices shown in Fig. 3, current sharing among the devices was predicted for different module currents. Shown in Fig. 6 is the predicted sharing curve between the MOSFETs and the diodes along with experimental data obtained from the bi-directional converter at three coolant temperatures. The I-V curve indicates that the MOSFET will conduct 100% of the module current below 40 A. At higher currents the MOSFET conducts 55% of the module current. The experimental MOSFET current was measured directly and showed that the MOSFET conducted a slightly higher current proportion (60%) than predicted. Furthermore, current sharing was found to be independent of the coolant temperature.

Next, the bi-directional converter circuit was simulated using the predicted current sharing to determine the losses in the MOSFET and the diode. There is minimal switching loss in the MOSFET since the device voltage is very small during MOSFET transitions. Therefore, the loss in each device was determined by estimating the conduction loss of the devices during typical buck operation when operating as the free-wheeling path.

These simulation results demonstrated two distinct benefits for employing the MOSFET in reverse conduction. The first was an increase in efficiency as the loss experienced in the switch was estimated to decrease 40-50% when exercising the MOSFET in reverse. The second benefit was additional output power capability of the converter. When only using the JBS diode as free-wheeling path, the output power of the converter was limited to 7.4 kW due to high diode temperatures. When the MOSFET is conducting in reverse the output power could be safely increased three-fold to 22.5 kW.

V. EXPERIMENTAL RESULTS

Experiments using the bi-directional converter with the diode only and both the diode and MOSFET in reverse conduction were done using coolant loop temperatures of 25 °C, 50 °C, and 80 °C. The input voltage to the converter (V_{HS}) was varied from 30 V to 260 V which produced S_2 module currents from 15 A_{RMS} to 138 A_{RMS} and resulted in output powers up to 22.5 kW. When operating in diode only mode, the output power was limited to 7.4 kW because the diode temperature would have exceeded the maximum allowable junction temperature of 200 °C at the next higher operating condition.

Fig. 7 shows the current waveforms for the maximum operating point while using the diode only for free-wheeling. The power in this case was limited by the diode temperature to 7.4 kW. One item to note is that current flowed through the SiC DMOSFET even when the device was off due to the parasitic body diode. The body diode initially took a portion of the module current, and then settled to a lower value after the SiC JBS diode was sufficiently biased.

Fig. 8 shows the current waveforms for the maximum operating point with both the JBS diode and MOSFET conducting which produced a peak module current of approximately 250 A. The inductor current increased while S_1 conducted, after which the SiC JBS diode turned on and conducted most of the current during the switching dead time

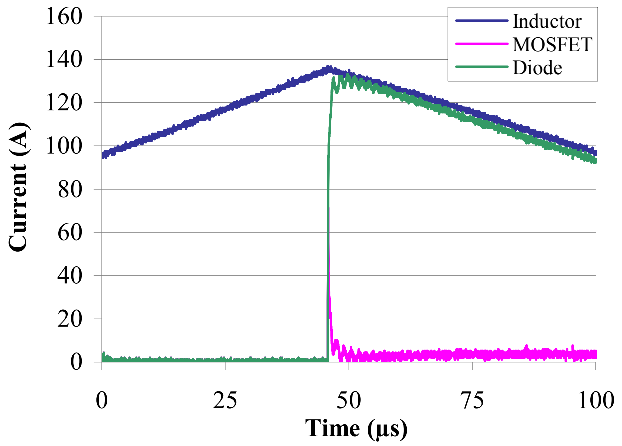

Figure 7: Current Waveforms at 7.4 kW Operation without Reverse Conduction and 80 °C Coolant.

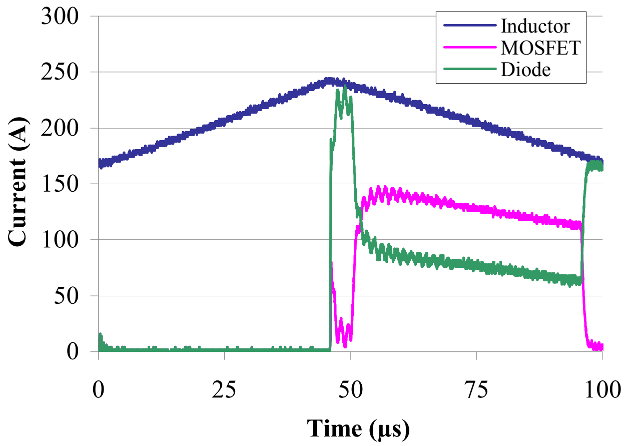

Figure 8: Current Waveforms at 22.5 kW Operation with Reverse Conduction and 80 °C Coolant.

TABLE I. EXPERIMENTAL RESULTS AT THREE COOLANT TEMPERATURES SHOWING DEVICE LOSSES WHILE UTILIZING THE MOSFET IN REVERSE AND USING THE DIODE ONLY

		25°C Coolant			50°C Coolant			80°C Coolant		
Output Power (kW)	*Module Current (A_{RMS})*	*MOSFET & DIODE Loss (W)*	*Diode Only Loss (W)*	*Reduction in Loss (%)*	*MOSFET & Diode Loss (W)*	*Diode Only Loss (W)*	*Reduction in Loss (%)*	*MOSFET & Diode Loss (W)*	*Diode Only Loss (W)*	*Reduction in Loss (%)*
1.1	30.9	26.9	33.8	20.4	25.0	31.9	21.7	27.6	35.2	21.7
2.9	49.5	46.0	61.8	25.6	45.1	62.6	28.0	48.2	70.6	31.7
5.1	65.3	66.8	101.6	34.2	65.3	106.2	38.5	71.8	122.2	41.2
7.4	78.8	87.5	154.8	43.5	87.0	165.7	47.5	96.9	195.4	50.4
10.1	92.6	113.0	Not attainable due to excessive diode temperatures		113.4	Not attainable due to excessive diode temperatures		126.4	Not attainable due to excessive diode temperatures	
13.2	106.0	144.3			145.9			163.9		
17.6	121.8	190.8			193.2			221.1		
22.5	137.5	248.7			256.1			293.6		

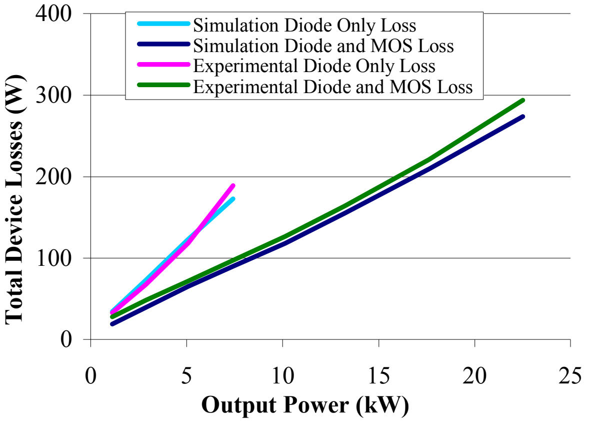

Figure 9: Device Loss vs. Output Power at 80 °C Coolant.

of 4.8 μs. The MOSFET current showed similar characteristics as before, taking some of the initial current spike and then settling to a low value as the body diode shared current with the JBS diode. After the dead time, S_2 turned on and current was shared between the SiC JBS diode and the SiC DMOSFET which was in reverse conduction.

Fig. 9 shows both the experimental and simulation data for the device losses at each operating point while operating at 80 °C coolant. As predicted by the simulation, losses in the module were reduced by 50% at higher power levels, although benefits at lower power levels are not as significant. Coolant temperature does have some effect on efficiency gain as observed in Table I, which summarizes the results from all of the experiments. Maximum benefits for reverse conduction occur at higher coolant temperatures.

VI. CONCLUSION

This paper documents a two-fold system-level benefit achieved by utilizing the reverse conduction mode of operation of a 100 A SiC DMOSFET module. The first benefit, decreased device losses, was shown through a bi-directional converter utilizing a complementary switching scheme. Experimental and simulation results demonstrated reduced power loss in the free-wheeling path by 30-50% achieved by a reverse conduction scheme. The second benefit was an increase in output power capability achieved by reducing device temperatures. The output power capability of the experimental module was increased from 7.4 kW while in diode only operation, to 22.5 kW while utilizing the reverse conduction ability of the MOSFET.

REFERENCES

[1] T.E. Salem, D.P. Urciuoli, R. Green, and G.K. Ovrebo, “High-Temperature High-Power Operation of a 100 A SiC DMOSFET Module,” *24th Annual IEEE Applied Power Electronics Conference and Exposition*, 2009, pp. 653-657.

[2] J. M. Miller, “Power Electronics in Hybrid Electric Vehicle Applications,” 18th *Annual IEEE Applied Power Electronics Conference and Exposition*, 2003, Vol. 1, pp. 23-29.

[3] A. Emadi, Y. J. Lee, and K. Rajashekara, “Power Electronics and Motor Drives in Electric, Hybrid Electric, and Plug-In Electric Vehicles,” *IEEE Transactions on Idustrial Electronics*, vol. 55, no. 6, pp. 2237-2245, June 2008.

[4] Hybrid Electric, and Plug-In Hybrid Electric Vehicles,” *IEEE Transactions on Industrial Electronics*, Vol. 55, No. 6, 2008, pp. 2237-2245.

[5] H. Zhang, L. M. Tolbert, and B. Ozpineci, “Impact of SiC Devices on Hybrid Electric and Plug-in Hybrid Electric Vehicles,” *IEEE Industry Applications Society Annual Meeting*, 2008, pp. 1-5

[6] M. Shen and F. Z. Peng, “Converter Systems for Hybrid Electric Vehicles,” *Proceeding of International Conference on Electrical Machines and Systems 2007*, 2007, pp. 2004-2010.

[7] A. Saplin, A. Meintz, and M. Ferdowsi, “Parametric Study of Alternative EV1 Powertrains,” *IEEE Vehicle Power and Propulsion Conference*, 2008, pp. 1-5.

[8] K. Acharya, S. K. Mazumder, and P. Jedraszczak, “Efficient, High-Temperature Bidirectional Dc/Dc Converter for Plug-in-Hybrid Electric Vehicle (PHEV) using SiC Devices,” *24th Annual IEEE Applied Power Electronics Conference and Exposition*, 2009, pp. 642-648.

[9] J. Lai and D.J. Nelson, “Energy Management Power Converters in Hybrid Electric and Fuel Cell Vehicles,” *Proceedings of the IEEE*, Vol. 95, No. 4, April 2007, pp. 766-777.

[10] D. P. Urciuoli, R. A. Wood, T. E. Salem, and G. K. Ovrebo, “Design and Development of a 400A, All Silicon-Carbide Power Module,” *NDIA-MI 2008 Ground-Automotive Power & Energy Workshop*, 2008.

[11] B. Baliga, *Fundamentals of Power Semiconductor Devices*, Springer, 2008.

[12] T. Funaki, M. Matsushita, M. Sasagawa, T. Kimoto, and T. Hikihara, “A Study on SiC Devices in Synchronous Rectification of DC-DC Converter,” *22th Annual IEEE Applied Power Electronics Conference and Exposition*, 2007, pp. 339-344.